

Change Point Detection for Random Objects using Distance Profiles

Paromita Dubey^{*1} and Minxing Zheng¹

¹Department of Data Sciences and Operations, Marshall School of Business,
University of Southern California

Abstract

We introduce a new powerful scan statistic and an associated test for detecting the presence and pinpointing the location of a change point within the distribution of a data sequence where the data elements take values in a general separable metric space (Ω, d) . These change points mark abrupt shifts in the distribution of the data sequence. Our method hinges on distance profiles, where the distance profile of an element $\omega \in \Omega$ is the distribution of distances from ω as dictated by the data. Our approach is fully non-parametric and universally applicable to diverse data types, including distributional and network data, as long as distances between the data objects are available. From a practical point of view, it is nearly tuning parameter-free, except for the specification of cut-off intervals near the endpoints where change points are assumed not to occur. Our theoretical results include a precise characterization of the asymptotic distribution of the test statistic under the null hypothesis of no change points and rigorous guarantees on the consistency of the test in the presence of change points under contiguous alternatives, as well as for the consistency of the estimated change point location. Through comprehensive simulation studies encompassing multivariate data, bivariate distributional data and sequences of graph Laplacians, we demonstrate the effectiveness of our approach in both change point detection power and estimating the location of the change point. We apply our method to real datasets, including U.S. electricity generation compositions and Bluetooth proximity networks, underscoring its practical relevance.

1 Introduction

With origins dating back to the 1950s (Page 1954, 1955), change point analysis has remained a thriving research area in statistics fueled by its burgeoning relevance in diverse domains such

^{*}Research supported in part by NSF grant DMS-2311034.

as biology and medicine (Oliver et al. 2004; Chung and Maisto 2006; Erdman and Emerson 2008; Kwon et al. 2008; Muggeo and Adelfio 2010; Picard et al. 2011; Shen and Zhang 2012; Sato et al. 2016), economics and finance (Lavielle and Teyssiere 2007; Barnett and Onnela 2016; Thies and Molnár 2018; Barassi et al. 2020), neurosciences (Lindquist et al. 2007; Stoehr et al. 2021; Cribben and Yu 2017), social sciences (Kossinets and Watts 2006; Sharpe et al. 2016; Wang et al. 2017), climate and environmental studies (Jaiswal et al. 2015; Lund et al. 2023), and more recently in the context of COVID-19 (Dehning et al. 2020; Jiang et al. 2023), to name but a few; see (Chen and Gupta 2012; Aminikhanghahi and Cook 2017; Truong et al. 2020) for recent reviews. The primary objective of change point detection is to identify and precisely locate any abrupt alteration in the data generating mechanism within an observed data sequence. Let the data sequence, indexed by time or another meaningful order, be represented as Y_1, \dots, Y_n . We consider the offline scenario, where the data sequence is of fixed length. A change point, denoted as n_τ , is characterized by the transition from the distribution P_1 governing Y_1, \dots, Y_{n_τ} to another distribution P_2 governing $Y_{n_\tau+1}, \dots, Y_n$ where $P_1 \neq P_2$.

In cases where the observations Y_i reside in the Euclidean space \mathbb{R}^p , the problem’s intricacies are influenced by the choice of the dimensionality p . While the univariate scenario has been thoroughly studied (Carlstein et al. 1994; Niu et al. 2016; Wang et al. 2020), additional challenges encountered in the multivariate case have triggered developments in both parametric (Srivastava and Worsley 1986; James et al. 1987, 1992; Csörgö and Horváth 1997; Zhang et al. 2010) as well as non-parametric frameworks (Matteson and James 2014; Lung-Yut-Fong et al. 2015; Jirak 2015; Madrid Padilla et al. 2022; Londschién et al. 2023). In the high-dimensional setting, the problem becomes significantly more intricate and elusive due to the curse of dimensionality. Specialized investigations targeting high-dimensional scenarios have emerged, including works by Wang and Samworth (2018); Enikeeva and Harchaoui (2019); Liu et al. (2021); Wang et al. (2022).

In modern data science, it is becoming increasingly common to encounter data that do not lie in a Euclidean space. Such data elements, often referred to as “random objects”, extend the traditional concept of random vectors into the realm of general metric spaces. Common examples include brain networks (Sporns 2022), gene regulation networks (Nie et al. 2017), linguistic object data (Tavakoli et al. 2019), distributional data (Matabuena et al. 2021), compositional data (Gloor et al. 2016), phylogenetic trees datasets (Holmes 2003; Kim et al. 2020) and many more. The bottleneck in working with such data lies in the absence of standard vector space operations, leaving us primarily with pairwise distances between these objects as our basis for analysis.

Methods to tackle change point analysis in these settings have evolved simultaneously. In addition to approaches designed for special cases like network data (Peel and Clauset 2015a; Jeong et al. 2016; Wang et al. 2021; Chen et al. 2023), distributional sequences (Horváth et al. 2021), compositional data (KJ et al. 2021) etc, which are not applicable more generally, there has been a surge in fully non-parametric approaches that can be placed in one of the three broad categories: distance-based (Matteson and James 2014; Li 2020; Chakraborty and Zhang 2021), kernel-based (Harchaoui and Cappé 2007; Harchaoui et al. 2008; Li et al. 2015; Garreau and Arlot 2018; Arlot et al. 2019; Chang et al. 2019) and graph-based (Chen and Zhang 2015; Shi et al. 2017; Nie and Nicolae 2021; Chen and Chu 2023). Nevertheless, each category of methods has its own set of limitations. In the case of kernel-based methods, critical decisions such as

choosing the appropriate kernel and setting parameters like bandwidth and penalty constants can significantly impact their effectiveness but are often challenging to determine in practice. On the other hand, the performance of graph-based methods is highly contingent on choosing from various graph construction methods, a choice that is often difficult to make. Recently, [Dubey and Müller \(2020\)](#) proposed a tuning free approach based on Fréchet means and variances in general metric spaces, however this test is not powerful against changes beyond Fréchet means and variances of the data.

In this paper, we propose a non-parametric, tuning parameter free (except for a cut-off interval at the end-points where change points are assumed not to occur) offline change point detection method for random objects based on distance profiles ([Dubey et al. 2022](#)), where the distance profile of a data element is the distribution of distances from that element as governed by the data. This new off-the-shelf method comes with rigorous type I error control, even when using permutation cutoffs, together with guaranteed consistency under contiguous alternatives. For fixed alternatives, we establish an optimal rate of convergence (up to log terms) for the estimated change point and also devise analogous rates of convergence under contiguous alternatives. We demonstrate the broad applicability and exceptional finite-sample performance of our method through extensive simulations covering various types of multivariate data, bivariate distributional data, and network data across a variety of scenarios. We illustrate our method on two real-world datasets: Bluetooth proximity networks in the MIT reality mining study and U.S. electricity generation compositional data.

The organization of the paper is as follows. In [Section 2](#), we delve into the problem’s setup, introducing the distance profiles and presenting our scan statistic. [Section ??](#) is dedicated to laying out the theoretical foundations of our proposed test, including a precise characterization of the asymptotic distribution of the scan statistic under the null hypothesis of no change points, analysis of the power of the test under contiguous alternatives and establishing rates of convergence for the estimated change point. Moving on to [Section 3](#), we introduce the various simulation settings, offering a comprehensive exploration of different types of random objects and change points scenarios. The performance of our test is illustrated in real-world applications, namely, the MIT Reality Mining networks and the U.S. electricity generation compositional data, in [Section 4](#). Finally, in [Section 5](#), we discuss the capacities of this new method, limitations and avenues for future extensions. In particular, we explore in depth the adaptation of our method utilizing seeded binary segmentation ([Kovács et al. 2023](#)) to scenarios involving multiple change points, which we illustrate using the set up of stochastic block models with multiple change points.

2 Methodology

2.1 Distance profiles of random objects

Distance profile, introduced in [Dubey et al. \(2022\)](#), is a simple yet powerful device for analyzing random objects in metric spaces. Let (Ω, d) be a separable metric space. Consider a probability space $(S, \mathcal{S}, \mathbb{P})$, where \mathcal{S} is the Borel sigma algebra on a domain S and \mathbb{P} is a probability measure.

A random object X is a measurable function, $X : S \rightarrow \Omega$ and P is a Borel probability measure on Ω that is induced by X , i.e. $P(A) = \mathbb{P}(\{s \in S : X(s) \in A\}) =: \mathbb{P}(X \in A) = \mathbb{P}(X^{-1}(A)) =: \mathbb{P} \circ X^{-1}(A)$, for any Borel measurable set $A \subseteq \Omega$. For any point $\omega \in \Omega$ its distance profile is the cumulative distribution function (cdf) of the distance between ω and the random object X that is distributed according to P . Formally we define the distance profile at ω as

$$F_\omega(t) = \mathbb{P}(d(\omega, X) \leq t), t \in \mathbb{R}.$$

We suppress the dependence of F_ω on P to keep the notation simple. Intuitively, if an element ω is more centrally located, i.e. closer to most other elements, it will have a distance profile with more mass near 0 unlike points which are distantly located from the data. With a sequence of independent observations X_1, \dots, X_n from P , we estimate the distance profile at ω as

$$\hat{F}_\omega(t) = \frac{1}{n} \sum_{j=1}^n \mathbb{I}\{d(\omega, X_j) \leq t\}, t \in \mathbb{R}.$$

The collection of the distance profiles $\{F_\omega : \omega \in \Omega\}$ comprises the one-dimensional marginals of the stochastic process $\{d(\omega, X)\}_\omega \in \Omega$ and serve as distinctive descriptors of the underlying Borel probability measure P whenever P can be characterized uniquely by open balls. Under special conditions on (Ω, d) , for example if d^r is of strong negative type for some $r > 0$ (Lyons 2013), this unique characterization holds for all Borel probability measures; see Proposition 1 in Dubey et al. (2022). Motivated by the new two-sample inference framework introduced in Dubey et al. (2022) our objective is to leverage these elementary distance profiles for detecting change points in the intricate distribution of a random object sequence.

2.2 Change point detection problem

Let Y_1, Y_2, \dots, Y_n be a sequence of random objects taking values in a separable metric space (Ω, d) with a finite covering number. Given two different Borel probability measures P_1 and P_2 on Ω , we will test the null hypothesis,

$$H_0 : Y_1, Y_2, \dots, Y_n \sim P_1 \tag{2.1}$$

against the single change point alternative

$$H_1 : \exists \tau \in (0, 1) \text{ such that } \begin{cases} Y_1, Y_2, \dots, Y_{[n\tau]} \sim P_1 \\ Y_{[n\tau]+1}, Y_{[n\tau]+2}, \dots, Y_n \sim P_2 \end{cases} \tag{2.2}$$

where τ denotes the change point. Our aim is to test the above hypothesis and accurately identify τ when it exists. In keeping with traditional change point methods, we will employ a scan statistic that involves dividing the data sequence into two segments, one before and one after the potential change points. In this process, the test statistic seeks to maximize the dissimilarities between these segments enabling subsequent inference and estimation of the change points if any. We quantify the dissimilarity between the data segments using the recently proposed two sample

test statistic based on distance profiles in [Dubey et al. \(2022\)](#) which is tuning parameter free and targets a divergence between the underlying population distributions in large samples (refer to the quantity D_{XY}^w in [Dubey et al. \(2022\)](#)) whenever the distributions are such that they can be uniquely identified using the distance profiles corresponding to all the elements in Ω .

To ensure the validity of large-sample analysis, it is important that both segments contain a minimum number of observations so that we can accurately capture the dissimilarity between them. Consequently, we make the assumption that the change point τ lies in a compact interval $\mathcal{I}_c = [c, 1 - c] \subset [0, 1]$, for some $c > 0$.

2.3 Scan statistic and type I error control

While scanning the data sequence segmented at $u \in \mathcal{I}_c$, let $\hat{F}_{Y_i}^{(u)}(t)$ be the estimated distance profile of the observation Y_i with respect to the data segment $Y_1, \dots, Y_{[nu]}$ given by

$$\hat{F}_{Y_i}^{(u)}(t) = \frac{1}{[nu]} \sum_{i=1}^{[nu]} \mathbb{I} \{d(Y_i, Y_j) \leq t\}, \quad t \in \mathbb{R}.$$

and $\hat{F}_{Y_i}^{(1-u)}(t)$, defined in a similar way with respect to the data segment $Y_{[nu]+1}, \dots, Y_n$, is given by

$$\hat{F}_{Y_i}^{(1-u)}(t) = \frac{1}{(n - [nu])} \sum_{i=[nu]+1}^n \mathbb{I} \{d(Y_i, Y_j) \leq t\}, \quad t \in \mathbb{R}.$$

To capture the discrepancy between the data segments $Y_1, \dots, Y_{[nu]}$ and $Y_{[nu]+1}, \dots, Y_n$ we use the statistic given by

$$\hat{T}_n(u) = \frac{[nu](n - [nu])}{n} \left\{ \frac{1}{n} \sum_{i=1}^n \int_0^{\mathcal{M}} (\hat{F}_{Y_i}^{(u)}(t) - \hat{F}_{Y_i}^{(1-u)}(t))^2 dt \right\} \quad (2.3)$$

where $\mathcal{M} = \text{diam}(\Omega)$ is the diameter of Ω . The motivation to investigate this scan statistic is that if the two segments $Y_1, \dots, Y_{[nu]}$ and $Y_{[nu]+1}, \dots, Y_n$ have different distributions, then the centrality of an observation Y_i , as encoded in the distance profiles, will be different across the two segments, and as a result $\hat{T}_n(u)$ tends to be large when u is close to τ when the change point τ exists. We demonstrate this using a toy example in [Figure 1](#). Hence to test the null hypothesis H_0 [\(2.1\)](#), we will use the test statistic

$$\hat{T}_n = \sup_{u \in \mathcal{I}_c} \hat{T}_n(u) = \max_{[nc] \leq k \leq n - [nc]} \hat{T}_n \left(\frac{k}{n} \right). \quad (2.4)$$



Figure 1: The distance profiles of Y_{200} in the sequence of observations Y_i , $i = 1, \dots, 300$, where $Y_i \sim N(0, 1)$, $i = 1, \dots, 100$ and $Y_i \sim N(2, 1)$, $i = 101, \dots, 300$ with respect to $Y_1, \dots, Y_{[nu]}$ and $Y_{[nu]+1}, \dots, Y_n$ at different scan points $u = \frac{1}{6}, \frac{1}{3}$ (the change point), $\frac{1}{2}, \frac{3}{4}$.

In order to construct an asymptotic level α test we derive the distribution of the test statistic (2.4) under H_0 (2.1) in Theorem 1 which needs the following assumptions.

- (A1) Let $F_\omega^{(1)}(t) = \mathbb{P}(d(\omega, Y) \leq t)$, where $Y \sim P_1$, and $F_\omega^{(2)}(t) = \mathbb{P}(d(x, Y') \leq t)$, where $Y' \sim P_2$. Assume that $F_\omega^{(1)}(t)$ and $F_\omega^{(2)}(t)$ are absolutely continuous for each $\omega \in \Omega$, with densities given by $f_\omega^{(1)}(t)$ and $f_\omega^{(2)}(t)$ respectively. Assume that there exists $L_1, L_2 > 0$ such that $\sup_{\omega \in \Omega} \sup_{t \in \mathbb{R}} |f_\omega^{(1)}(t)| \leq L_1$ and $\sup_{\omega \in \Omega} \sup_{t \in \mathbb{R}} |f_\omega^{(2)}(t)| \leq L_2$. Moreover assume that $\inf_{t \in \text{supp}(f_\omega^{(1)})} f_\omega^{(1)}(t) > 0$ and $\inf_{t \in \text{supp}(f_\omega^{(2)})} f_\omega^{(2)}(t) > 0$ for each $\omega \in \Omega$.
- (A2) Let $N(\epsilon, \Omega, d)$ be the covering number of the space Ω with balls of radius ϵ and $\log N(\epsilon, \Omega, d)$ the corresponding metric entropy, which satisfies

$$\epsilon \log N(\epsilon, \Omega, d) \rightarrow 0 \quad \text{as} \quad \epsilon \rightarrow 0. \quad (2.5)$$

Assumption (A1) imposes regularity conditions on the distance profiles under the distributions P_1 and P_2 . Assumption (A2) constrains the complexity of the metric space (Ω, d) and is applicable to a wide range of spaces including any space Ω which can be represented as a subset of elements in a finite dimensional Euclidean space, for example networks (Kolaczyk et al. 2020; Ginestet et al. 2017), simplex valued objects in a fixed dimension (Jeon and Park 2020; Chen et al. 2012) and the space of phylogenetic trees with the same number of tips (Kim et al. 2020; Billera et al. 2001). Assumption (A2) holds for any Ω which is a VC-class of sets or a VC-class of functions (Theorems 2.6.4 and 2.6.7, Van Der Vaart et al. 1996), for p -dimensional smooth function classes $C_1^\alpha(\mathcal{X})$ (page 155, Van Der Vaart et al. 1996) on bounded convex sets \mathcal{X} in \mathbb{R}^p equipped with the $\|\cdot\|_\infty$ -norm (Theorem 2.7.1, Van Der Vaart et al. 1996) and $\|\cdot\|_{r,Q}$ -norm for any probability measure Q on \mathbb{R}^p (Corollary 2.7.2, Van Der Vaart et al. 1996) if $\alpha \geq p+1$ and for the case when Ω is the space of one-dimensional distributions on some compact interval $I \subset \mathbb{R}$ that are absolutely continuous with respect to the Lebesgue measure on I with smooth uniformly bounded densities and $d = d_W$ with d_W being the 2-Wasserstein metric (Dubey et al. 2022). In fact Assumption (A2) is satisfied when Ω is the space of p -dimensional distributions on a compact convex set

$I \subset \mathbb{R}^p$, represented using their distribution functions endowed with the L_r metric with respect to the Lebesgue measure on I if $\Omega \subset C_1^\alpha(I)$ for $\alpha \geq p + 1$. Next we present Theorem (1) which establishes the null distribution of the test statistic (2.4) as $n \rightarrow \infty$ as the law of the random variable \mathcal{T} as introduced in the same theorem.

Theorem 1. *Under H_0 and assumptions (A1) and (A2), as $n \rightarrow \infty$, \hat{T}_n converges in distribution to the law of a random variable $\mathcal{T} = \sup_{u \in \mathcal{I}_c} \sum_{j=1}^{\infty} \mathbb{E}_Y \{\lambda_j^Y\} \mathcal{G}_j^2(u)$, where $Y \sim P_1$, $\lambda_1^x \geq \lambda_1^y \geq \dots$ correspond to the eigenvalues of the covariance function given by $C_x(t_1, t_2) = \text{Cov}(\mathbb{I}\{d(x, Y) \leq t_1\}, \mathbb{I}\{d(x, Y) \leq t_2\})$ and $\mathcal{G}_1, \mathcal{G}_2, \dots$ are independent zero mean Gaussian processes with covariance given by $c(u_1, u_2) = \sqrt{\frac{(1-u_1)(1-u_2)}{u_1 u_2}} \min(u_1, u_2) + \sqrt{\frac{u_1 u_2}{(1-u_1)(1-u_2)}} \min(1 - u_1, 1 - u_2)$.*

Here we discuss the major bottleneck that we needed to overcome in proving Theorem 1 and relegate the technical details to the Supplement. Since the goal is to have a sample-splitting free test, we use the same observations Y_1, \dots, Y_n to estimate the distance profiles and thereafter to estimate the scan statistic that makes each summand in (2.3) significantly dependent on each other. To obtain the null distribution in Theorem 1 we decompose the test statistic (2.4) into several parts, some of which contribute to the asymptotic null distribution while we that the others are asymptotically negligible using maximal inequalities from U-process theory.

For a level α test, we propose to reject H_0 (2.1) if $\hat{T}_n > q_\alpha$ where q_α is the $(1 - \alpha)$ -quantile of \mathcal{T} . Equivalently one rejects H_0 when $p \leq \alpha$ where $p = \mathbb{P}_{H_0}(\mathcal{T} \geq \hat{T}_n)$ is the asymptotic p value of the test. Unfortunately, the law of \mathcal{T} depends on the underlying data distribution and the rejection region, either using the critical value q_α or the p value p must be approximated in practice. Staying in line with adopted conventions we adopt a random permutation scheme to obtain this approximation that is described next and later design a framework in Section 2.4 to study the power of the test using this approximation scheme in large samples.

Let Π denote the collection of $n!$ permutations of $\{1, 2, \dots, n\}$. Let $\pi_0 = (\pi_0(1), \dots, \pi_0(n))$ be the identity permutation such that $\pi_0(j) = j$ for $j = 1, \dots, n$ and $\pi_1, \pi_2, \dots, \pi_K$ be K i.i.d samples from the uniform distribution over Π where each $\pi_k = (\pi_k(1), \dots, \pi_k(n))$ is a permutation of $\{1, \dots, n\}$. For each $k = 0, 1, 2, \dots$, let $\hat{T}_n^{\pi_k}$ be the test statistic evaluated on a reordering of the data given by $Y_{\pi_k(1)}, \dots, Y_{\pi_k(n)}$. Then the permutation p value is given by $\hat{p}_K = \frac{1}{K+1} \sum_{k=0}^K \mathbb{I}\left\{\hat{T}_n^{\pi_k} \geq \hat{T}_n\right\}$ and the test is rejected at level α when $\hat{p}_K \leq \alpha$. It is easy to see that under H_0 (2.1), \hat{p}_K as an approximation of p controls the type I error of the test at level α with high probability for sufficiently large K (see Chung and Romano (2016)).

2.4 Power analysis under contiguous alternatives

We will study the large sample power of the test, first assuming that the asymptotic critical value q_α is available, and thereafter using the practicable permutation scheme for the test. A few definitions are in order before we can state our results. For $t \in \mathbb{R}$ and a random object Y , where it is possible that either $Y \sim P_1$ or $Y \sim P_2$, let $F_Y^{(1)}(t) = \mathbb{P}_{Y'}(d(Y, Y') \leq t)$ with $Y' \sim P_1$ and

$F_Y^{(2)}(t) = \mathbb{P}_{Y''}(d(Y, Y'') \leq t)$ with $Y'' \sim P_2$ and both Y' and Y'' are independent of Y . Define the quantity $\Delta = \Delta(P_1, P_2)$ as

$$\Delta = \mathbb{E}_{Y \sim P_1} \left(\int_0^{\mathcal{M}} \left\{ F_Y^{(1)}(t) - F_Y^{(2)}(t) \right\}^2 dt \right) + \mathbb{E}_{Y \sim P_2} \left(\int_0^{\mathcal{M}} \left\{ F_Y^{(1)}(t) - F_Y^{(2)}(t) \right\}^2 dt \right) \quad (2.6)$$

where $\mathcal{M} = \text{diam}(\Omega)$ is the diameter of Ω . Immediately one sees that under H_0 (2.1), $\Delta = 0$. In fact Δ corresponds to the quantity D_{XY}^w introduced in Dubey et al. (2022) and under mild conditions (Ω, d) , P_1 and P_2 , $\Delta = 0$ if and only if $P_1 = P_2$.

Let $\mathcal{P}_{(\Omega, d)}$ denote the class of all Borel probability measures on (Ω, d) which are uniquely determined by open balls, that is, for $Q_1, Q_2 \in \mathcal{P}_{(\Omega, d)}$, $Q_1 = Q_2$ if and only if $F_{\omega}^{Q_1}(t) = F_{\omega}^{Q_2}(t)$ for all $\omega \in \Omega$ and $t \in \mathbb{R}$. In fact $\mathcal{P}_{(\Omega, d)}$ contains all Borel probability measures on (Ω, d) under special conditions on (Ω, d) such as, for example, when (Ω, d^k) is of strong negative type (Lyons 2013) for some $k > 0$ (see Proposition 1 in Dubey et al. (2022)). Then $\Delta = 0$ implies that $F_{\omega}^{P_1}(u) = F_{\omega}^{P_2}(u)$ for almost any $t \in \mathbb{R}$ and for any ω in the union of the supports of P_1 and P_2 . Hence if Ω is contained in the union of the supports of P_1 and P_2 , then $\Delta = 0$ implies that $P_1 = P_2$ whenever $P_1, P_2 \in \mathcal{P}_{(\Omega, d)}$ in which case Δ serves as a divergence measure between P_1 and P_2 and can be used to measure the discrepancy between H_1 (2.2) and H_0 (2.1).

To investigate the power of the test we consider the challenging case, a sequence of alternatives $H_{1,n}$ that shrinks to H_0 where

$$H_{1,n} = \{(P_1, P_2) : \Delta = a_n\} \quad (2.7)$$

with $a_n \rightarrow 0$ as $n \rightarrow \infty$. In this framework the asymptotic power of a level α test is quantified using

$$\beta_n^\alpha = \mathbb{P}_{H_{1,n}}(p \leq \alpha)$$

where p is the asymptotic p-value and depends on the null distribution of the test described by the law of \mathcal{T} in Theorem 1. Since the law of \mathcal{T} is unknown, we obtain a tractable estimator of p given by \hat{p}_K using the permutation scheme, and the practicable power is quantified as

$$\tilde{\beta}_n^\alpha = \mathbb{P}_{H_{1,n}}(\hat{p}_K \leq \alpha). \quad (2.8)$$

Theorem 2 gives the asymptotic consistency for any level α test, by showing that the power of the test in both asymptotic and practicable regimes converge to one as $n \rightarrow \infty$ in the hard to detect scenario of contiguous alternatives provided that $na_n \rightarrow \infty$, i.e., a_n does not decay too fast as $n \rightarrow \infty$.

Theorem 2. *Under assumptions (A1) and (A2), for any $\alpha \in (0, 1)$ and as $n \rightarrow \infty$, $\beta_n^\alpha \rightarrow 1$ as $n \rightarrow \infty$. Moreover if $na_n \rightarrow \infty$ and $K \geq \frac{1}{\alpha}$, where K is the total number of permutations used to estimate \hat{p}_K in (2.8) then $\tilde{\beta}_n^\alpha \rightarrow 1$ as $n \rightarrow \infty$.*

2.5 Change point estimation

In this section we describe the estimation of τ when it exists. As a straightforward consequence of our test statistic (2.4) we estimate τ as

$$\hat{\tau} = \arg \max_{u \in \mathcal{I}_c} \hat{T}_n(u). \quad (2.9)$$

Next we discuss the asymptotic behavior of $\hat{\tau}$ around τ . For this we consider two scenarios, first, where the alternative is fixed which is the case that is studied typically in nonparametric change point analysis, and then the case where the alternative is such that $(P_1, P_2) \in H_{1,n}$ with $H_{1,n}$ as defined in (2.7) such that $\Delta(P_1, P_2) = a_n$ with $a_n \rightarrow 0$ as $n \rightarrow \infty$. The second scenario offers a difficult setup for detecting τ accurately. In Theorem 3 we show the asymptotic near-optimal rate of convergence for the change point in the first scenario of fixed alternatives when $P_1 \neq P_2$ (Madrid Padilla et al. 2021). In the second situation, the change point estimator $\hat{\tau}$ is a consistent estimator of τ only if $na_n \rightarrow \infty$ as $n \rightarrow \infty$, which is also the requirement for the consistency of the test as per Theorem 2.

Theorem 3. *For any fixed alternative when $P_1 \neq P_2$, under assumptions (A1) and (A2), as $n \rightarrow \infty$,*

$$|\hat{\tau} - \tau| = O_P\left(\frac{\log(n)}{n}\right).$$

For the contiguous alternatives $H_{1,n}$, there exists $L > 0$ such that $\mathbb{P}_{H_{1,n}}(na_n|\hat{\tau} - \tau| \geq L) \rightarrow 0$ as $n \rightarrow \infty$.

3 Simulations

We assess the finite sample performance of our approach across various frameworks involving three different random object spaces. First we carry out extensive simulations capturing diverse change point scenarios in sequences of Euclidean random vectors, then we study change points in bivariate distributional data sequences where the bivariate distributions are equipped with the L^2 metric between corresponding the cdfs, and finally move on to change points in random network sequences where the networks are represented as graph Laplacians with the Frobenius metric between them and are generated from a preferential attachment model (Barabási and Albert 1999). For each random object we explore a range of alternatives beyond location shifts and scale shifts, such as, sudden changes in the tails of the population distribution, the population distribution abruptly switching to a mixture distribution with two components and abrupt changes in network node attachment mechanisms.

We generate random object sequences of length $n = 300$ and set the level α of the test to be $\alpha = 0.05$. In each scenario, we first calibrate the type I error of the new test under H_0 and then evaluate the empirical power of the test for a succession of alternatives that capture increasing discrepancies between the distributions of the two data segments before and after the change point with $\tau = 1/3$. We employ our scan statistic on the interval $\mathcal{I}_c = [0.1, 0.9]$. We conduct 500 Monte

Carlo runs and set the empirical power to be the proportion of the rejections at $\alpha = 0.05$ out of the 500 Monte Carlo runs. The critical value of is approximated using the permutation scheme described in Section 2.3 with 1000 permutations within each Monte Carlo run. To demonstrate our findings we present empirical power plots where we expect that the empirical power will be maintained at the level $\alpha = 0.05$ under H_0 and will increase with increasing disparities between the the two data segments. Along with the power trends we also investigate the accuracy of the estimated change point locations using their mean absolute deviation (MAE), calculated as

$$\text{MAE} = \frac{1}{500} \sum_{i=1}^{500} |\hat{\tau}_i - \tau|,$$

where $\hat{\tau}_i$ is the estimated change point location in the i -th Monte Carlo run. We expect that a successful method will have better accuracy in detecting change points, and therefore, have lower MAE with higher distributional differences between the data segments.

We compare the power and the MAE of our test statistic, which we will refer to as “dist-CP” here on, with the energy-based change point detection test (“energy-CP”)(Matteson and James 2014), graph-based change point detection test (“graph-CP”)(Chen and Zhang 2015; Chu and Chen 2019), and kernel-based change point detection test (“kernel-CP”) (Harchaoui et al. 2008; Jones and Harchaoui 2020). We adopt the same configuration whenever needed for each of these tests, for example, we set the number of permutations to be 1000 to obtain the p-value approximations. For the graph-based test, we apply the generalized edge-count scan statistic (Chu and Chen 2019) and choose 5-MST (minimum spanning tree) to construct the initial similarity graph as suggested by Chen and Zhang (2015). For the kernel-CP, we use the Gaussian kernel and select the bandwidth to be the median of the input pairwise distances. In terms of the implementation, we use the R packages “gSeg”(?) and “ecp”(?) for graph-CP and energy-CP separately, and Python package “Chapydette”(Jones and Harchaoui 2020) for kernel-CP.

3.1 Multivariate data

In this setting the data elements are random vectors endowed with l^2 metric and are generated from the p -dimensional Gaussian distribution $N(\mu, \Sigma)$ with mean μ and covariance matrix given by Σ . We explore four different types of changes to the population distributions, which we summarize in Table 1. First we consider location and scale changes, in dimensions $p = 30, 90$ and 180 where to study location change, we set $\mu = \mathbf{0}_p = (0, 0, \dots, 0)^T$ for Y_i , $i = 1, \dots, 100$ and $\mu = \Delta_1 \mathbf{1}_p = \Delta_1(1, 1, \dots, 1)^T$ for Y_i , $i = 101, \dots, 300$, where we let Δ_1 range from 0 to 1. The covariance matrix is fixed and constructed as $\Sigma = U\Lambda U^T$, where Λ is a diagonal matrix with k -th diagonal entry being $\cos(k\pi/p) + 1.5$ for $k = 1, \dots, p$, and U is an orthogonal matrix with the first columns being $p^{-1/2}(1, 1, \dots, 1)^T$, such that the mean change loads along the first eigenvector of the data. To investigate scale change, we fix the $\mu = \mathbf{0}_p$ and set $\Sigma = 0.8\mathbf{I}_p$ for Y_i , $i = 1, \dots, 100$ and $\Sigma = (0.8 - \Delta_2)\mathbf{I}_p$ for Y_i , $i = 101, \dots, 300$, where we let Δ_2 range from 0 to 0.4. We present the results of location and scale shifts in Figure 2, where Figure 2a illustrates the empirical power performances of the tests and Figure 2b shows the MAE of estimated change

points. In Figure 3, we present the corresponding results for scale change. In Figure 2a, we see that all the methods maintain type I error control. Energy-CP outperforms the other methods in terms of power and MAE but dist-CP has competitive power performance across all different settings in the mean change scenario. For scale changes, dist-CP has the best performance in terms of both empirical power and MAE across all settings as illustrated in Figure 3.

$P_1 (Y_1, \dots, Y_{100} \sim P_1)$	$P_2 (Y_{101}, \dots, Y_{300} \sim P_2)$
$N(\mathbf{0}_p, \Sigma)$ with $\Sigma = Q\Lambda Q^T$, where Λ is a diagonal matrix with i th entry $\cos(i\pi/p) + 1.5$ for $i = 1, \dots, p$ and Q is an orthogonal matrix whose first column is $p^{-1/2}(1, 1, \dots, 1)^T$	$N(\Delta_1 \mathbf{1}_p, \Sigma)$, where $\Delta_1 \in [0, 1]$
$N(\mathbf{0}_p, \Sigma)$, $\Sigma = 0.8\mathbf{I}_p$	$N(\mathbf{0}_p, \Sigma)$, where $\Sigma = (0.8 - \Delta_2)\mathbf{I}_p$ and $\Delta_2 \in [0, 0.4]$
$N(\mathbf{0}_p, \mathbf{I}_p)$	$AZ_1 + (1 - A)Z_2$, where $A \sim \text{Bernoulli}(0.5)$, $Z_1 \sim N(-\mu, \mathbf{I}_p)$, $Z_2 \sim N(\mu, \mathbf{I}_p)$, where $\mu = (\Delta_3 \mathbf{1}_{0.1p}, \mathbf{0}_{0.9p})^T$, where $\Delta_3 \in [0, 1]$ and A , Z_1 , and Z_2 are independent.
$N(\mathbf{0}_p, \mathbf{I}_p)$	p -dimensional random vectors whose components are independent and identically distributed as the t-distribution blue with v degrees of freedom, where $v \in \{2, \dots, 22\}$

Table 1: Different change point scenarios when $\Omega = \mathbb{R}^p$ equipped with metric $d = \|x - y\|_2$ for $x, y \in \Omega$. Going from top to bottom, the successive rows encode population mean change, population scale change, the population distribution separating into distinct mixture components and the population distribution changing to being heavy-tailed.

Next we study sudden splitting of a homogeneous population into a mixture of two components with different means. To study this we take Y_1, \dots, Y_{100} to be generated from the standard p -dimensional Gaussian distribution $N(\mathbf{0}_p, \mathbf{I}_p)$ and let Y_{101}, \dots, Y_{300} be generated from a mixture of two Gaussian distributions with the overall population mean same as Y_1, \dots, Y_{100} . To be more specific, Y_{101}, \dots, Y_{300} are constructed with independent samples of $AZ_1 + (1 - A)Z_2$, where $A \sim \text{Bernoulli}(0.5)$, $Z_1 \sim N(-\mu, \mathbf{I}_p)$, $Z_2 \sim N(\mu, \mathbf{I}_p)$, where $\mu = (\Delta_3 \mathbf{1}_{0.1p}, \mathbf{0}_{0.9p})^T$, and A , Z_1 , and Z_2 are independent. Here, $\Delta_3 \in [0, 1]$. In Figure 4 we illustrate that dist-CP outperforms all other approaches both in terms of empirical power and MAE in this complex change point scenario.

Finally we experiment with changes to the tail of the population distribution. We generate $Y_i \sim N(\mathbf{0}_p, \mathbf{I}_p)$ with $p \in \{5, 15, 60\}$ for $i = 1, \dots, 100$ and Y_i as a p -dimensional random vector whose components are independent and identically distributed as the t-distribution with v degrees of freedom for $i = 101, \dots, 300$. We let v range in $\{2, \dots, 22\}$ to reflect the change from Gaussian tails to successively heavier tails. The results as shown in Figure 5 demonstrate that dist-CP has the best power and MAE performance across all settings.

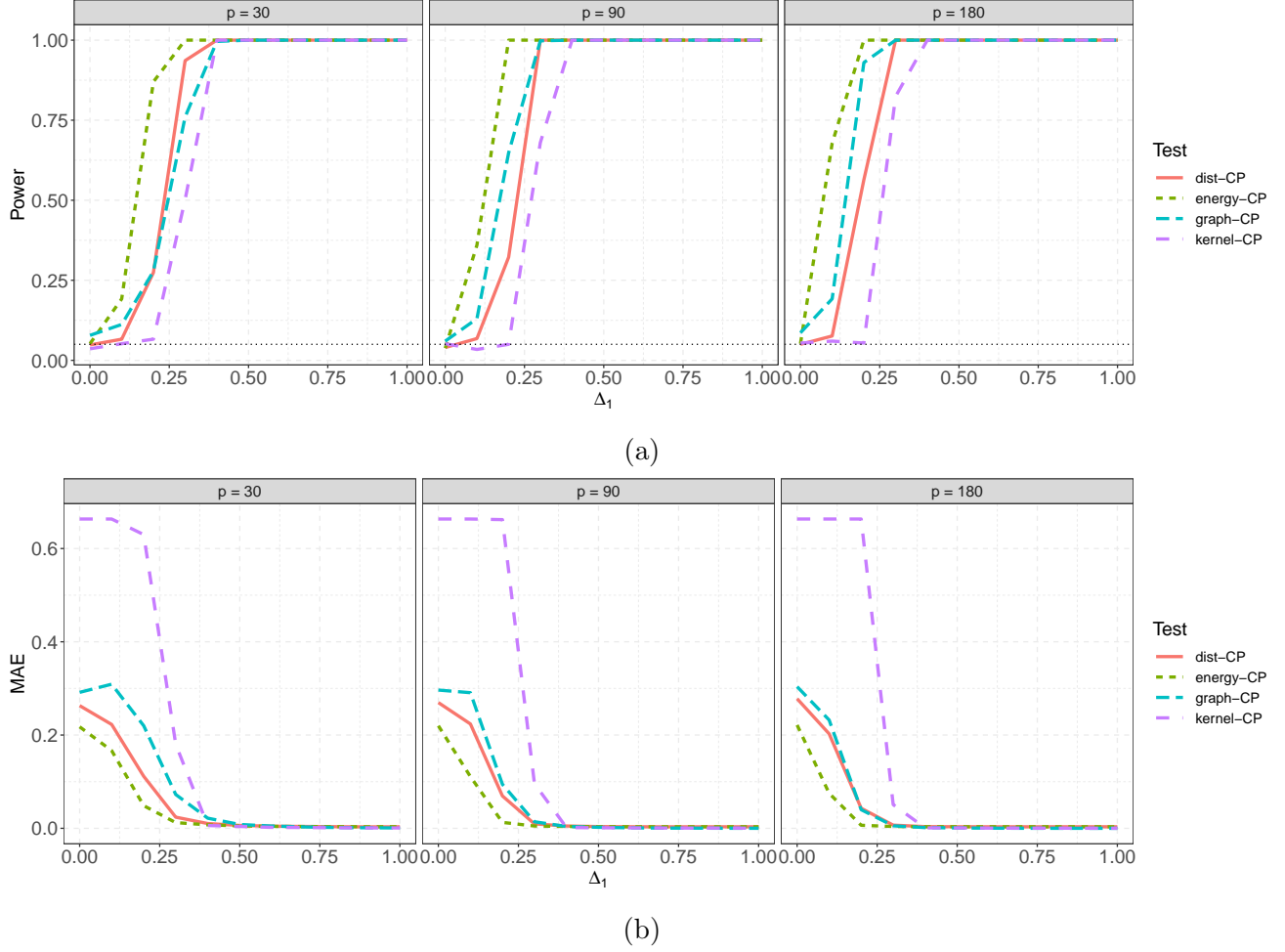
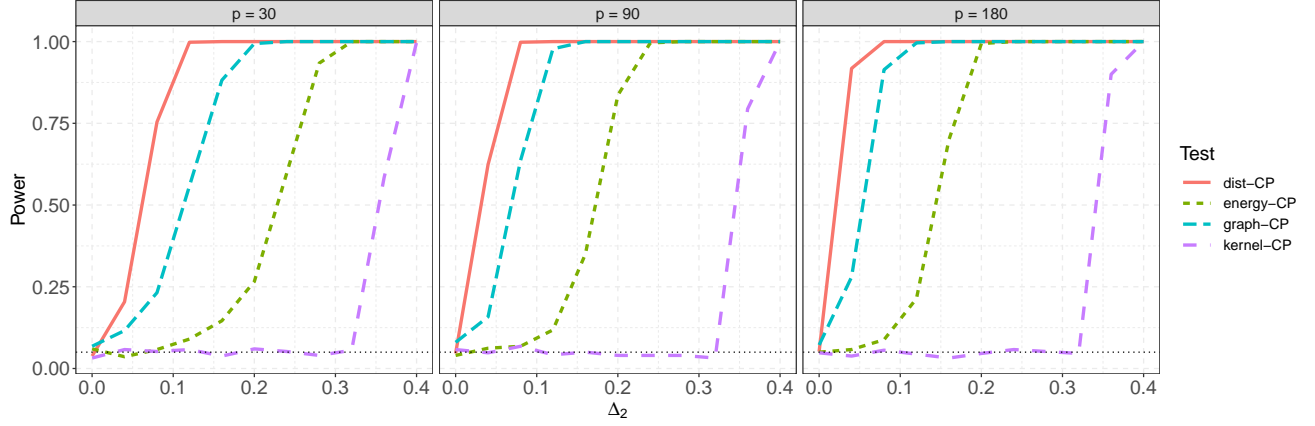
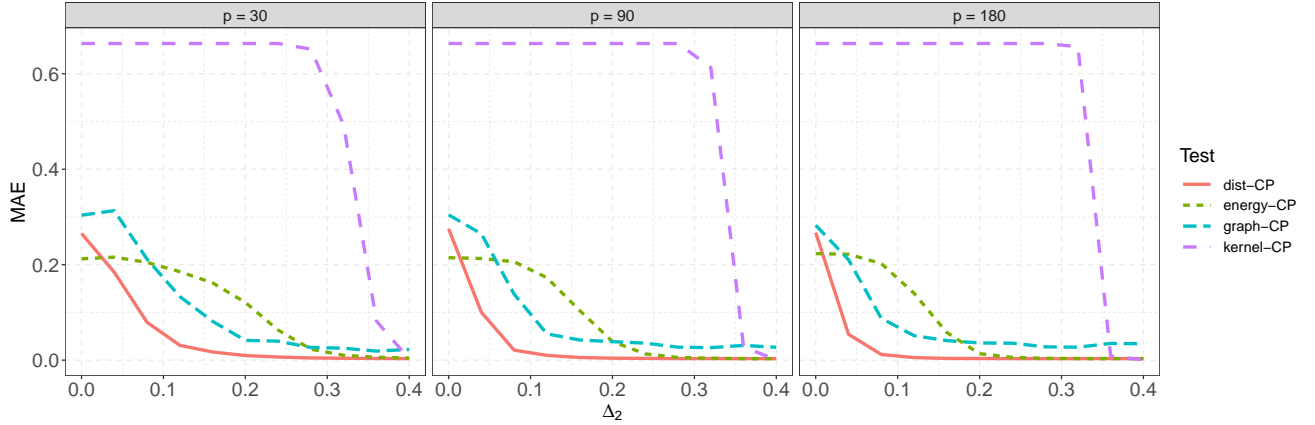


Figure 2: In Figure 2a, we present the power comparisons with respect to Δ_1 (see Table 1) for a sequence of p -dimensional random vectors sampled from $N(\mu, \Sigma)$, where $\mu = \mathbf{0}_p = (0, 0, \dots, 0)^T$ for Y_i , $i = 1, \dots, 100$ and $\mu = \Delta_1 \mathbf{1}_p = \Delta_1(1, 1, \dots, 1)^T$ for Y_i , $i = 101, \dots, 300$. Σ is held fixed for the whole sequence as $\Sigma = U\Lambda U^T$, where Λ is a diagonal matrix with k th diagonal entry being $\cos(k\pi/p) + 1.5$ for $k = 1, \dots, p$, and U is an orthogonal matrix with the first columns being $p^{-1/2}(1, 1, \dots, 1)^T$. The dotted black line indicates the significance level of 0.05. Figure 2b presents the MAE of the estimated change points with respect to Δ_1 .



(a)



(b)

Figure 3: In Figure 3a, we present the power comparisons with respect to Δ_2 (see Table 1) for a sequence of p - dimensional random vectors sampled from $N(\mu, \Sigma)$, where $\mu = \mathbf{0}_p$ for the whole sequence. $\Sigma = 0.8\mathbf{I}_p$ for Y_i , $i = 1, \dots, 100$ and $\Sigma = (0.8 - \Delta_2)\mathbf{I}_p$ for Y_i , $i = 101, \dots, 300$. The dotted black line indicates the significance level of 0.05. Figure 3b presents the MAE of the estimated change points with respect to Δ_2 .

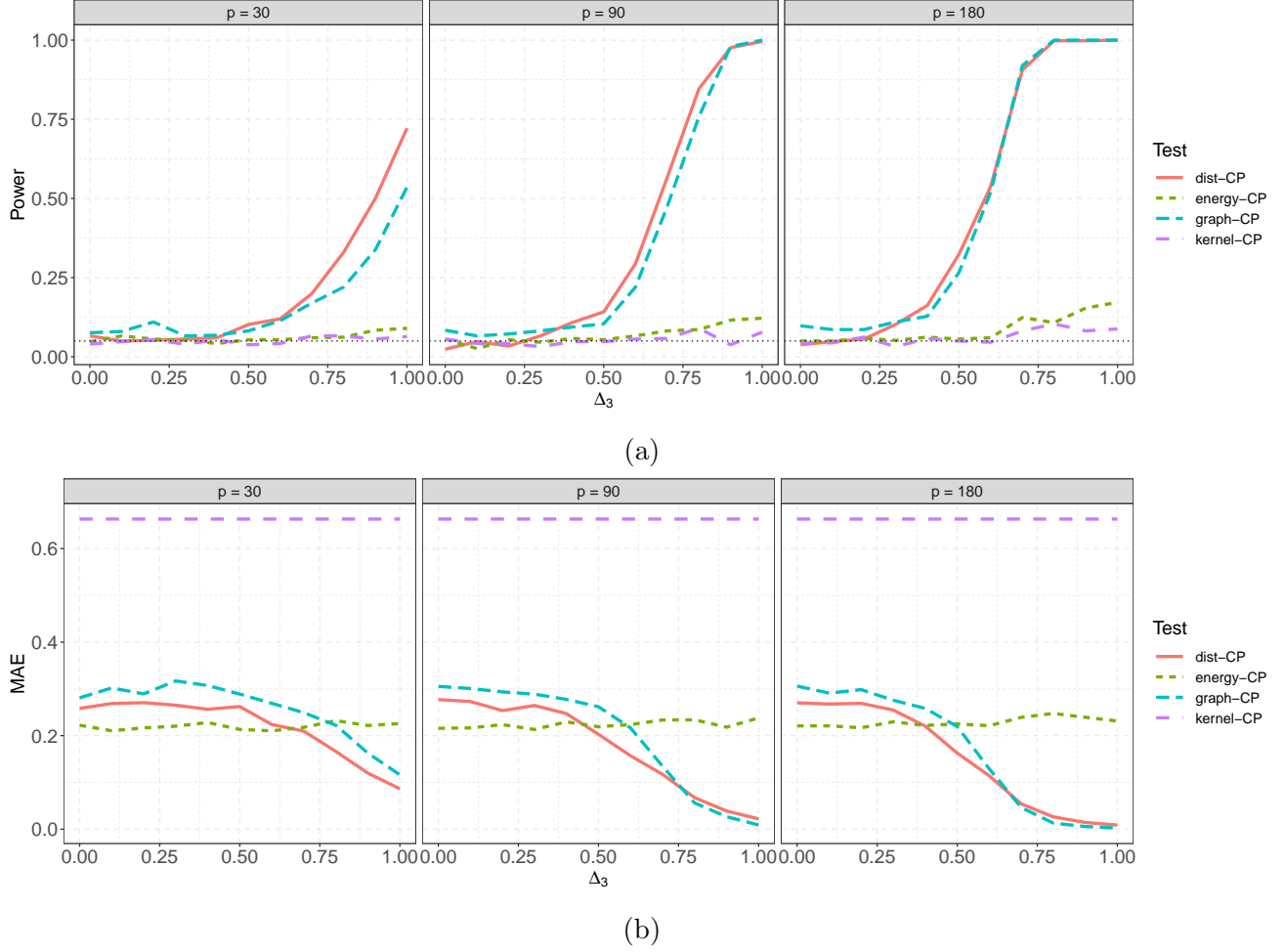
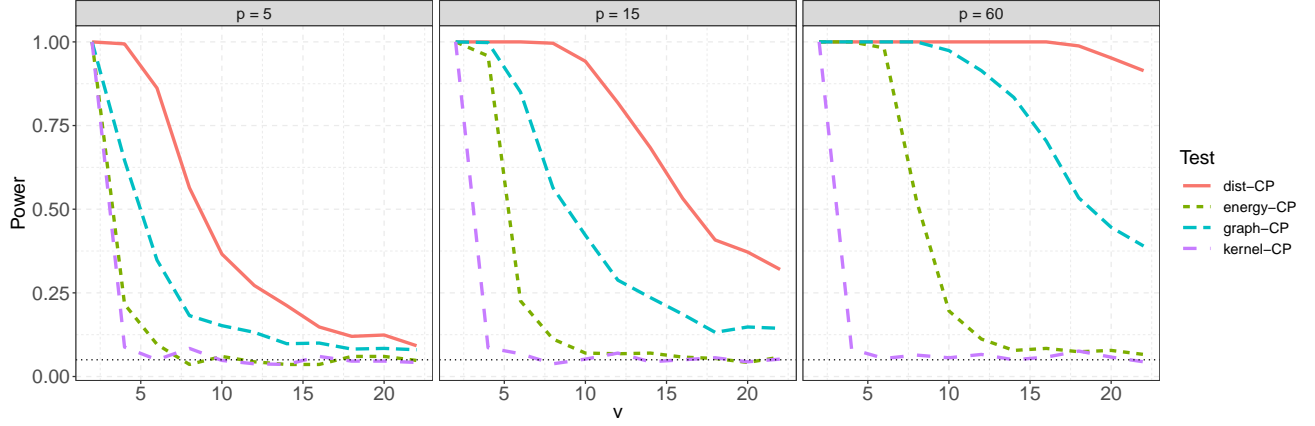
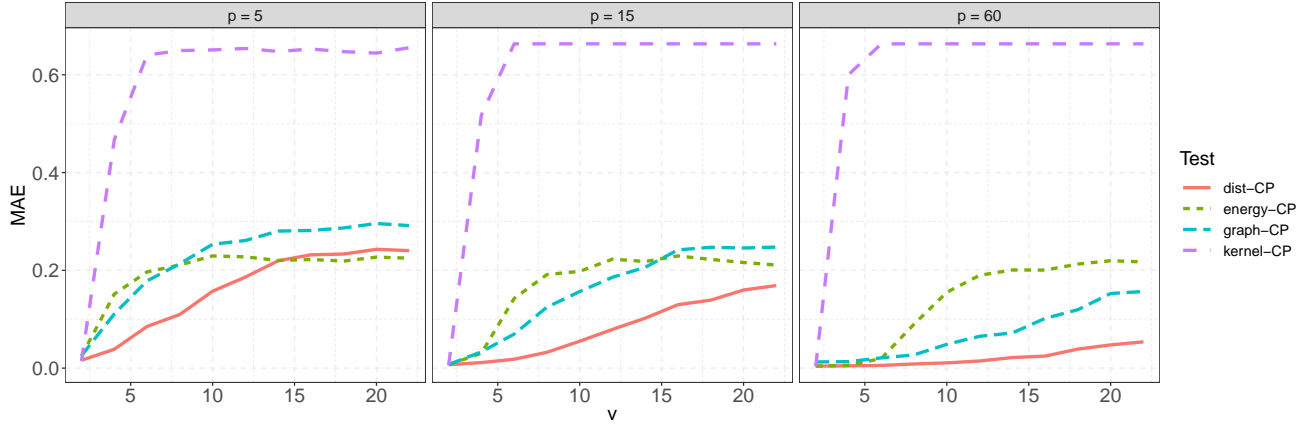


Figure 4: In Figure 4a, we present the power comparisons with respect to Δ_3 (see Table 1) for a sequence of p dimensional random vectors. Here, Y_1, \dots, Y_{100} are generated from the standard p dimensional Gaussian distribution $N(\mathbf{0}_p, \mathbf{I}_p)$. Y_{101}, \dots, Y_{300} are constructed with independent samples of $AZ_1 + (1 - A)Z_2$, where $A \sim \text{Bernoulli}(0.5)$, $Z_1 \sim N(-\mu, \mathbf{I}_p)$, $Z_2 \sim N(\mu, \mathbf{I}_p)$, where $\mu = (\Delta_3 \mathbf{1}_{0.1p}, \mathbf{0}_{0.9p})^T$, and A , Z_1 , and Z_2 are independent. The dotted black line indicates the significance level of 0.05. Figure 4b presents the MAE of the estimated change points with respect to Δ_3 .



(a)



(b)

Figure 5: In Figure 5a, we present the power comparison for increasing values of v (see Table 1) for a sequence of p dimensional random vectors. Here, $Y_i \sim N(\mathbf{0}_p, \mathbf{I}_p)$ with $p \in \{5, 15, 60\}$ for $i = 1, \dots, 100$ and $Y_i \sim t_v$ for $i = 101, \dots, 300$, where t_v stands for t distribution with v degrees of freedom. The dotted black line indicates the significance level of 0.05. Figure 5b presents the MAE of the estimated change points with respect to v .

3.2 Bivariate distributional data

Here the random objects are random bivariate probability distributions equipped with the metric between corresponding cumulative distribution function representations defined as $d(x, y) = \int_{\mathbb{R}} \int_{\mathbb{R}} |F_x(u, v) - F_y(u, v)| \, dudv$, where $F_x(u, v)$ is the bivariate cdf of x . Each observation Y_i for $i = 1, \dots, 300$ is itself a bivariate distribution with a cdf representation where we explore two types of changes: changes in the process generating the means of Y_i and changes in the process generating the variances in the covariance structure of Y_i . We provide a summary of the changes in Table 2. Specifically, for the first scenario, $Y_i = N(Z_i, 0.25\mathbf{I}_2)$, where $Z_i \sim N(\mathbf{0}_2, 0.25\mathbf{I}_2)$ for $i = 1, \dots, 100$, and $Z_i \sim N((\delta_1, 0)^T, 0.25\mathbf{I}_2)$ for $i = 101, \dots, 300$ where $\delta_1 \in [0, 1]$. For changes in the scales of the random distributions we generate $Y_i = N(Z_i, 0.25\mathbf{I}_2)$, where $Z_i \sim N(\mathbf{0}_2, 0.4^2\mathbf{I}_2)$ for $i = 1, \dots, 100$, and $Z_i \sim N(\mathbf{0}_2, \text{diag}((0.4 + \delta_2)^2, 0.4^2))$ for $i = 101, \dots, 300$ and let $\delta_2 \in [0, 4]$. We illustrate our findings in 6 and 7. In Figure 6, dist-CP, energy-CP, and kernel-CP have similar performance and are better than graph-CP in terms of both power and MAE. In the second case, dist-CP dominates the performance across all settings.

$P_1 (Y_1, \dots, Y_{100} \sim P_1)$	$P_2 (Y_{101}, \dots, Y_{300} \sim P_2)$
$Y_i = N(Z_i, 0.25\mathbf{I}_2)$ with $Z_i \sim N(\mathbf{0}_2, 0.25\mathbf{I}_2)$	$Y_i = N(Z_i, 0.25\mathbf{I}_2)$ with $Z_i \sim N((\delta_1, 0)^T, 0.25\mathbf{I}_2)$, and $\delta_1 \in [0, 1]$
$Y_i = N(Z_i, 0.25\mathbf{I}_2)$ with $Z_i \sim N(\mathbf{0}_2, 0.4^2\mathbf{I}_2)$	$Y_i = N(Z_i, 0.25\mathbf{I}_2)$ with $Z_i \sim N(\mathbf{0}_2, \text{diag}((0.4 + \delta_2)^2, 0.4^2))$, and $\delta_2 \in [0, 0.4]$

Table 2: Different change point scenarios for $\Omega = \{(u, v) \mapsto F(u, v) : F(\cdot, \cdot) \text{ is a bivariate cdf}\}$ equipped with the metric $d = \int_{\mathbb{R}} \int_{\mathbb{R}} |F_x(u, v) - F_y(u, v)| \, dudv$ for $F_x, F_y \in \Omega$. The first row describes a change in the distribution of the mean of each Y_i and the second row describes a change in the distribution of scale aspects of each Y_i .

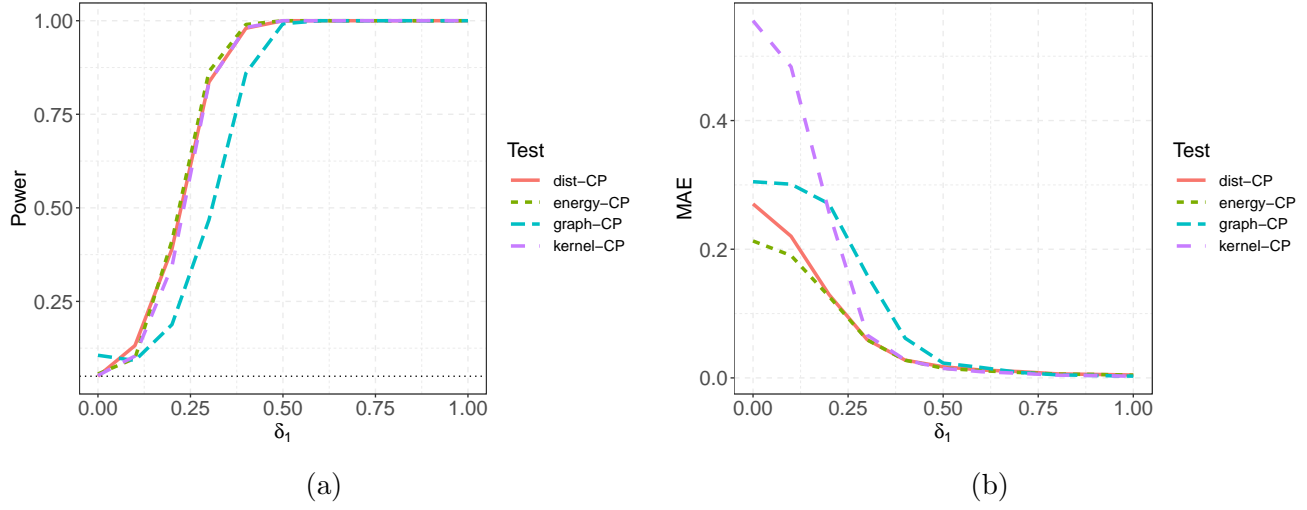


Figure 6: In Figure 6a, we present the power comparisons with respect to δ_1 (see Table 2) for a sequence of bivariate Gaussian distributional data. Here, $Y_i = N(Z_i, 0.25\mathbf{I}_2)$, where $Z_i \sim N(\mathbf{0}_2, 0.25\mathbf{I}_2)$ for $i = 1, \dots, 100$, and $Z_i \sim N((\delta_1, 0)^T, 0.25\mathbf{I}_2)$ for $i = 101, \dots, 300$. The dotted black line indicates the significance level of 0.05. Figure 6b presents the MAE of the estimated change points with respect to δ_1 .

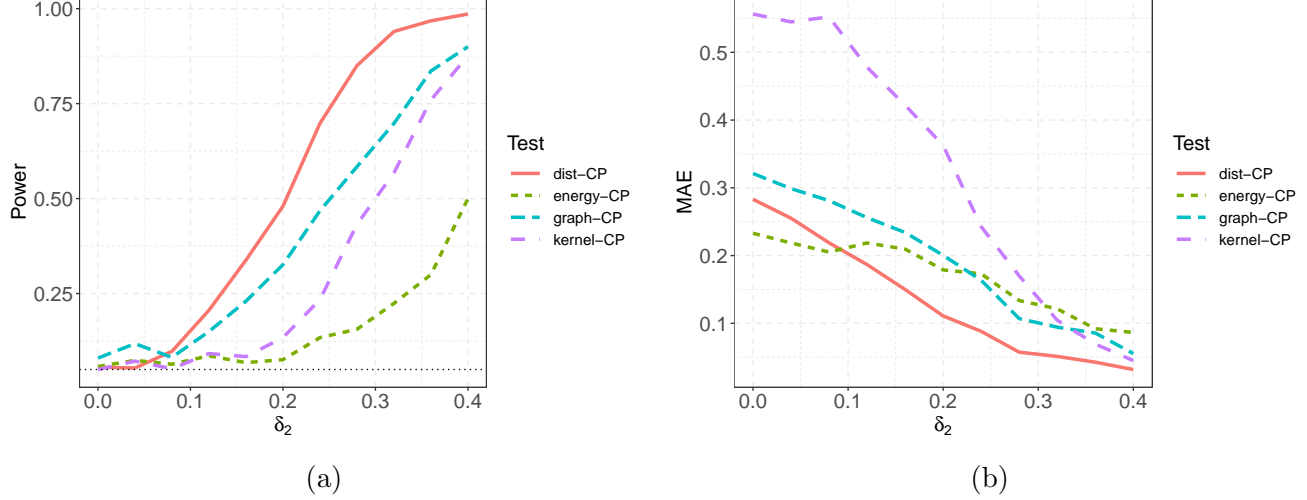


Figure 7: In Figure 7a, we present the power comparison for increasing values of δ_2 (see Table 2) for a sequence of bivariate Gaussian distributional data. Here, $Y_i = N(Z_i, 0.25\mathbf{I}_2)$, where $Z_i \sim N(\mathbf{0}_2, 0.4^2\mathbf{I}_2)$ for $i = 1, \dots, 100$, and $Z_i \sim N(\mathbf{0}_2, \text{diag}((0.4 + \delta_2)^2, 0.4^2))$ for $i = 101, \dots, 300$. The dotted black line indicates the significance level of 0.05. Figure 7b presents the MAE of the estimated change points with respect to δ_2 .

3.3 Network data

Lastly, we consider random object sequences where the data elements are random networks endowed with the Frobenius metric between the corresponding Laplacian matrix¹. Each Y_i is a network with 200 nodes generated from the preferential attachment model (Barabási and Albert 1999) where for a node with degree k , its attachment function is proportional to k^γ . Y_i is generated with $\gamma = 0$ for $i = 1, \dots, 100$, and Y_i is generated with γ from 0 to 0.5 for $i = 101, \dots, 300$. We summarize the settings in Table 3, and present the simulation results in Figure 8. dist-CP outperforms the other methods in both power and change point location estimation MAE.

P_1 ($Y_1, \dots, Y_{100} \sim P_1$)	P_2 ($Y_{101}, \dots, Y_{300} \sim P_2$)
networks generated from preferential attachment model with $\gamma = 0$	networks generated from preferential attachment model with $\gamma \in [0, 0.5]$

Table 3: Change point scenario where $\Omega = \{\text{graph laplacians of networks with 200 nodes}\}$ equipped with metric $d(L_1, L_2) = \sqrt{\text{trace}((L_1 - L_2)^T(L_1 - L_2))}$ for $L_1, L_2 \in \Omega$.

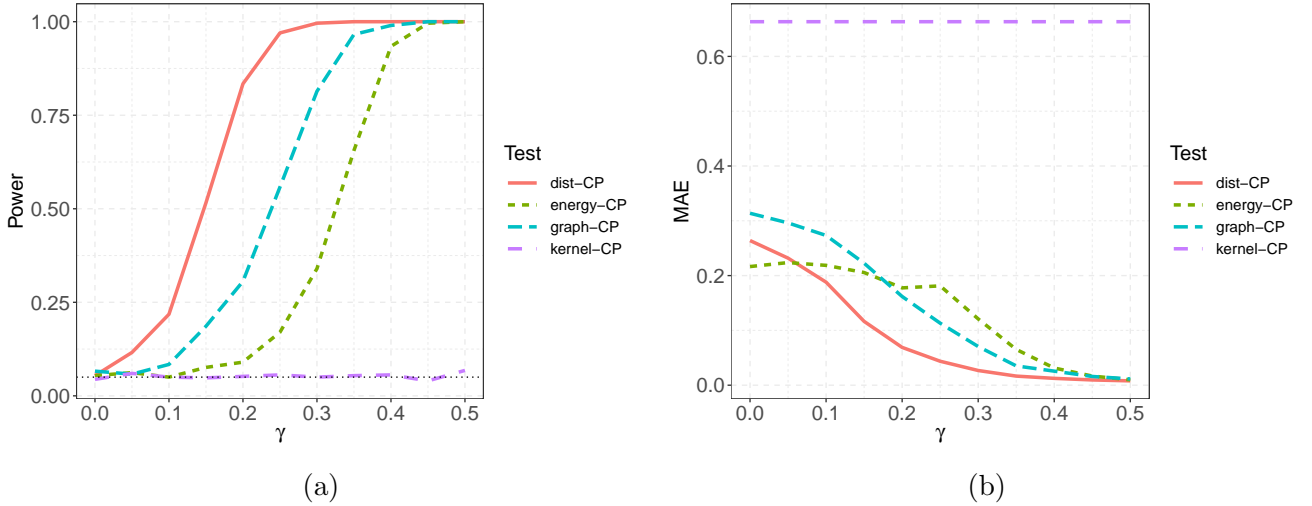


Figure 8: In Figure 8a, we present the power comparisons with respect to increasing values γ (see Table 3) for a sequence of random networks with 200 nodes generated by the preferential attachment model. For a node with degree k , its attachment function is proportional to k^γ . Y_i is generated with $\gamma = 0$ for $i = 1, \dots, 100$, and Y_i is generated with $\gamma \in [0, 0.5]$ for $i = 101, \dots, 300$. The dotted black line indicates the significance level of 0.05. Figure 8b presents the MAE of the estimated change points with respect to γ .

¹The graph Laplacian for a network is defined $L = D - A$ where D is the degree matrix (diagonal matrix spanned by node degrees) and A is the adjacency matrix.

4 Data applications

4.1 U.S. electricity generation dataset

We analyze the monthly U.S. electricity generation compositions obtained from <https://www.eia.gov/electricity/data/browser/>. We preprocess the data elements into a compositional form so that each entry of the compositional vector represents the percentage of net generation contribution from a specific source. During the preprocessing, we merge some similar categories of resources together and end up with 7 categories: Coal; Petroleum (petroleum liquids and petroleum coke); Gas (natural and other gases); Nuclear; Conventional hydroelectric; Renewables (wind, geothermal, biomass (total) and other); Solar (small-scale solar photovoltaic and all utility-scale solar). We obtain a sample of $n = 264$ observations starting from Jan 2001 to Dec 2022. Each Y_i takes values in a 6-simplex $\Delta^6 = \{\mathbf{x} \in \mathbb{R}^7 : \mathbf{x}^T \mathbf{1}_7 = 1\}$, where $\mathbf{1}_7 = (1, 1, \dots, 1)^T$. The metric we apply between each object is

$$d(\mathbf{x}, \mathbf{y}) = \arccos(\sqrt{\mathbf{x}}^T \sqrt{\mathbf{y}}), \quad \mathbf{x}, \mathbf{y} \in \mathbb{R}^7,$$

where $\sqrt{\mathbf{x}}$ is the component-wise square root, i.e., $\sqrt{\mathbf{x}} = (\sqrt{x_1}, \sqrt{x_2}, \dots, \sqrt{x_7})$.

We apply dist-CP to the preprocessed data and present the plot of the scan statistic in Figure 9. The scan statistic peaks in month of February 2015. In Figure 10, we present the statistically significant estimated change point location with a vertical red dash line. At the change point, we can observe that the percentage of contributions from solar and renewable sources is increasing more rapidly while petroleum contributions drop rapidly. U.S. reached new milestones in renewables electricity generation in the year 2015 (see <https://obamawhitehouse.archives.gov/blog/2016/01/13/renewable-electricity-progress-accelerated-2015>) which explains the detected change point.

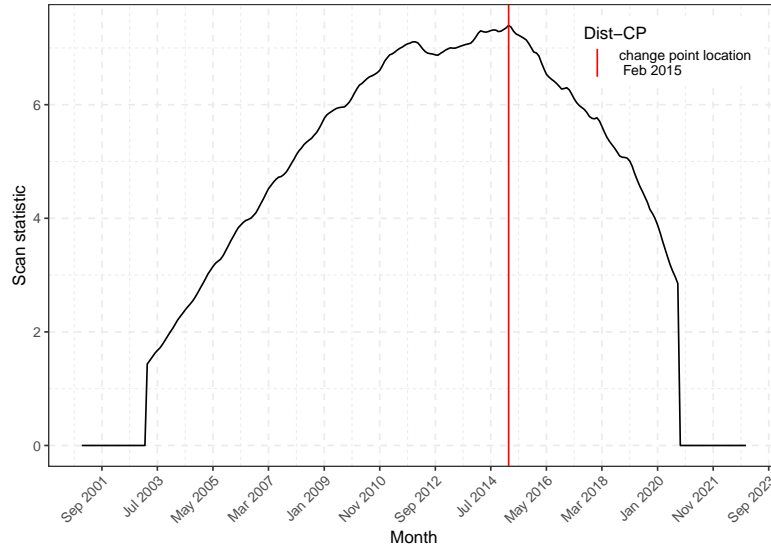


Figure 9: The scan statistic for the monthly U.S. electricity compositions data. The vertical red line indicates the location of the estimated change point in the month of February 2015.

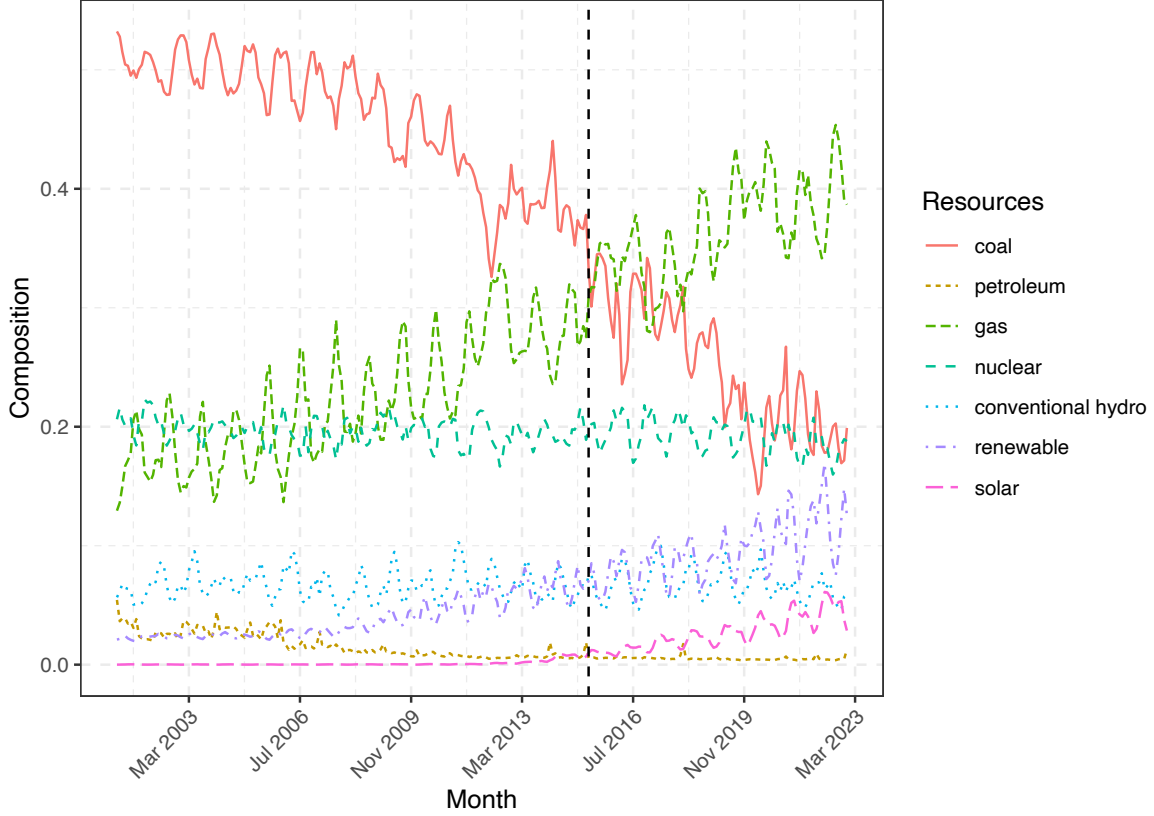


Figure 10: The timeline of U.S. electricity compositions evolution and the change point February 2015 indicated by the vertical dashed black line.

4.2 MIT reality mining dataset

The MIT Media Laboratory conducted the reality mining experiment from 2004 to 2005 on students and faculty at MIT (Eagle and Pentland 2006) in order to explore human interactions based on Bluetooth and other phone applications’ activities. We study the participants’ Bluetooth proximity networks, where nodes represent participants and the edges represent whether the relevant participants had at least one physical interaction within the time interval.

We use the reality mining 1392 built-in dataset in the R package “GreedySBTM” (?) (see https://github.com/cran/GreedySBTM/blob/master/data/reality_mining_1392.RData). The time frames corresponding to intervals of 4 hours, starting from September 14 2004 to May 5 2005. At each time point the network has = 96 nodes. We further compressed the data by merging the time windows with a day to obtain 232 daily networks. We work with the pairwise Frobenius metric between the graph Laplacian representation of the networks. Using dist-CP the estimated change point is 2004-12-15, which is during the finals week and close to the start of the winter break. We present the scan statistics for the whole sequence in Figure 11.

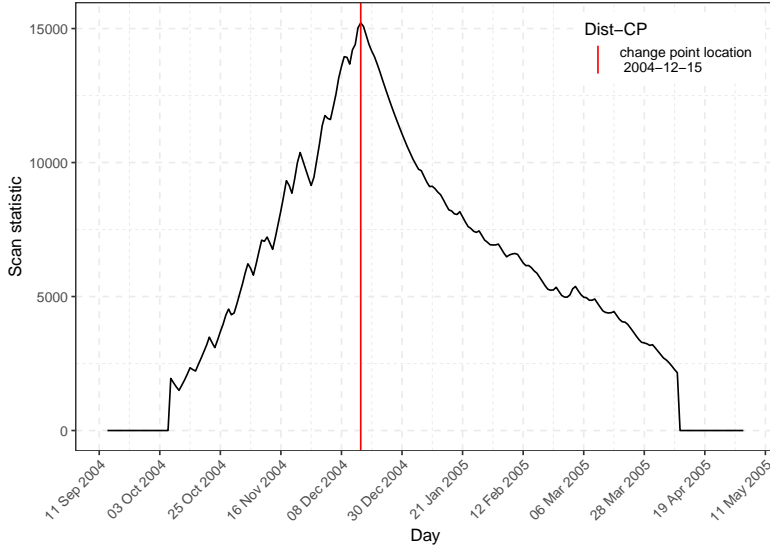


Figure 11: The scan statistic for MIT reality mining dataset. The vertical red line indicates the estimated change point 2004-12-15 which is during the finals week and around the beginning of the winter break.

5 Multiple change points

In this section, we investigate the extension of dist-CP to the task of detecting multiple change points. We combine our test statistic with the recently proposed seeded binary segmentation algorithm (Kovács et al. 2023), an approach that shares similar ideas with the wild binary segmentation (Fryzlewicz 2014). Seeded binary segmentation controls the computational cost in a near-linear time by creating a collection of seeded intervals \mathcal{I}_γ which removes unnecessarily long intervals in wild binary segmentation that might contain multiple change points. As introduced in Kovács et al. (2023), for a sequence of length n , the collection of intervals \mathcal{I}_γ is given by

$$\mathcal{I}_\gamma = \bigcup_{k=1}^{\lceil \log_{1/\gamma}(n) \rceil} \mathcal{I}_k \quad (5.1)$$

where $\gamma \in [1/2, 1)$ is a decay parameter, $\mathcal{I}_k = \bigcup_{i=1}^{n_k} \{(\lfloor (i-1)s_k \rfloor), \lfloor (i-1)s_k + l_k \rfloor\}$ and $n_k = 2\lceil (1/\gamma)^{k-1} \rceil - 1$. Each \mathcal{I}_k is also a collection of intervals of length l_k that are evenly shifted by s_k , where $l_k = n\gamma^{k-1}$, $s_k = (T - l_k)/(n_k - 1)$. In algorithm 1, we describe the detailed implementation of the Mcpd-DP, the multiple change point detection algorithm based on the combination of distance profiles and seeded binary segmentation. Once we obtain \mathcal{I}_γ , we conduct “dist-CP” on each of the inner intervals thus deriving a set of potential change point locations. We compare the test statistic in each inner interval of \mathcal{I}_γ with a threshold which is set at 90%-quantile of the permutation null distribution of the test statistic derived on the entire sequence in the current implementation. The selection rule is to keep intervals in which the test statistic is greater

than the above threshold and remove all the other intervals sequentially until the maximum test statistic in the entire collection of remaining intervals does not exceed the threshold. In the experiments, we set $\gamma = 1/2^{1/2}$ as suggested by Kovács et al. (2023) and set minLen to be 10.

Algorithm 1 Multiple change point detection based on distance profile: MCPD_DP

Input: l and u : lower and upper boundaries of the original sequence, minLen: minimum length of each interval, γ : decay parameter, initial change point set $\hat{\tau} = \emptyset$

Output: detected change point set $\hat{\tau}$

```

1: procedure MCPD_DP( $l, u, \gamma, \hat{\tau}, \text{minLen}$ )
2:   if  $u - l < \text{minLen}$  then STOP.
3:   calculate the seeded interval collection  $\mathcal{I}_\gamma$  as described in equation 5.1.
4:   for  $i$  in 1 to  $|\mathcal{I}_\gamma|$  do
5:     denote  $u_i$  and  $l_i$  the upper and lower boundaries of the  $i$ th interval in  $\mathcal{I}_\gamma$ .
6:     denote the proposed test statistics on interval  $[l_i, u_i]$  as  $\hat{T}_i$  and record its corresponding
       estimated change point location as  $\hat{t}_i$ 
7:   end for
8:   Let  $\Delta$  be the 90% quantile of the approximated permutation distribution based on the
       entire sample  $Y_1, \dots, Y_n$ .
9:   if  $\max_i \hat{T}_i \geq \Delta$  then
10:     $i' \leftarrow \operatorname{argmax}_{i \in \{1, \dots, |\mathcal{I}_\gamma|\}} \hat{T}_i$ 
11:     $\hat{\tau} \leftarrow \hat{\tau} \cup \hat{t}_{i'}$ 
12:    conduct MCPD_DP( $l, \hat{t}_{i'}, \gamma, \hat{\tau}, \text{minLen}$ ) and MCPD_DP( $\hat{t}_{i'}, u, \gamma, \hat{\tau}, \text{minLen}$ )
13:   else
14:     break
15:   end if
16: end procedure

```

5.1 Simulations on network sequences generated using the Stochastic Block Model

To demonstrate the practical efficacy of Mcdp_DP in Algorithm 1, we conduct an experiment on sequences of networks generated according to the stochastic block model (SBM). SBM generates networks with adjacency matrices $A = [A_{ij}] \in \mathbb{R}^{n \times n}$ with K communities, where $A_{ij} \sim \text{Bernoulli}(P_{ij})$ with $P = [P_{ij}] = \Pi B \Pi^T - \text{diag}(\Pi B \Pi^T)$. Here $\Pi \in \mathbb{R}^{n \times K}$ encodes the community membership of each node, that is, $\Pi_{ik} = 1$ if node i belongs to community k and $\Pi_{ik} = 0$ otherwise. Here $B \in \mathbb{R}^{K \times K}$ is the connection probability matrix, where B_{ij} indicates the connection probability between i -th and j -th community. We let $\pi \in \mathbb{R}^K$ to be such that π_i indicates the number of nodes in i -th community.

To incorporate different kinds of changes, we focus on the diverse characteristics of the SBM such as changes in the number of nodes in each community and changes in the number of communities. We generate a sequence of networks of length $n = 400$ in the SBM framework

with change points evenly spaced at $\tau = \{\frac{1}{4}, \frac{2}{4}, \frac{3}{4}\}$. Specifically Y_i are generated with $B = \begin{pmatrix} 0.2 & 0.001 & 0.001 \\ 0.001 & 0.2 & 0.001 \\ 0.001 & 0.001 & 0.2 \end{pmatrix}$, and $\pi = (100, 100, 100)$ for $1 \leq i \leq 100$. Then, we change the connecting probability to $B = \begin{pmatrix} 0.8 & 0.001 & 0.001 \\ 0.001 & 0.2 & 0.001 \\ 0.001 & 0.001 & 0.8 \end{pmatrix}$, and keep $\pi = (100, 100, 100)$ the same for $101 \leq i \leq 200$. Next, we change $\pi = (200, 50, 50)$ and keep B the same for $201 \leq i \leq 300$. Finally for $301 \leq i \leq 400$, we change the number of communities, we set $B = \begin{pmatrix} 0.5 & 0.01 \\ 0.01 & 0.5 \end{pmatrix}$ and $\pi = (200, 100)$.

We apply Mcpd_DP 1 on the network sequences generated according to the SBM framework described above, and compare the performance with the multiple change points version of energy-CP (Matteson and James 2014; ?) and kernel-CP (Arlot et al. 2019). We conduct 500 Monte Carlo runs and evaluate Algorithm 1 on two aspects; first, whether the correct number of change points can be detected and second, conditioning on the correctly estimating the number of change points, on the MAE of the estimated change points. Out of 500 Monte Carlo runs, the proportions of correctly estimating 3 change points are 100%, 95.8% and 100% for the proposed algorithm Mcpd_DP, energy-CP and kernel-CP. All of the three methods achieve zero MAE conditioning on correctly estimating the number of 3 points.

5.2 Multiple change points in real data

Next we illustrate the implementation of Mcpd_DP 1 on the real data examples investigated in Section 4. For the U.S. electricity generation data, Mcpd_DP detects May 2007, February 2015 and February 2019 as the change points as illustrated in Figure 12. In May 2007, while renewable sources pick up suddenly, the petroleum component starts a rapid downward trend alongside abrupt changes in the trends of the coal component. In February 2015 the solar component starts to accelerate along with continuing changes in the renewable component with similar change patterns again in February 2019. For MIT reality mining data, Mcpd_DP 1 detects change points at 2004-10-16 (beginning of sponsor week), 2004-12-16 (around the end of the finals week and beginning of the winter break), 2005-01-01 (starting of the independent activities period) and 2005-03-10 (right after the exam week) according to events labeled in Peel and Clauset (2015b).

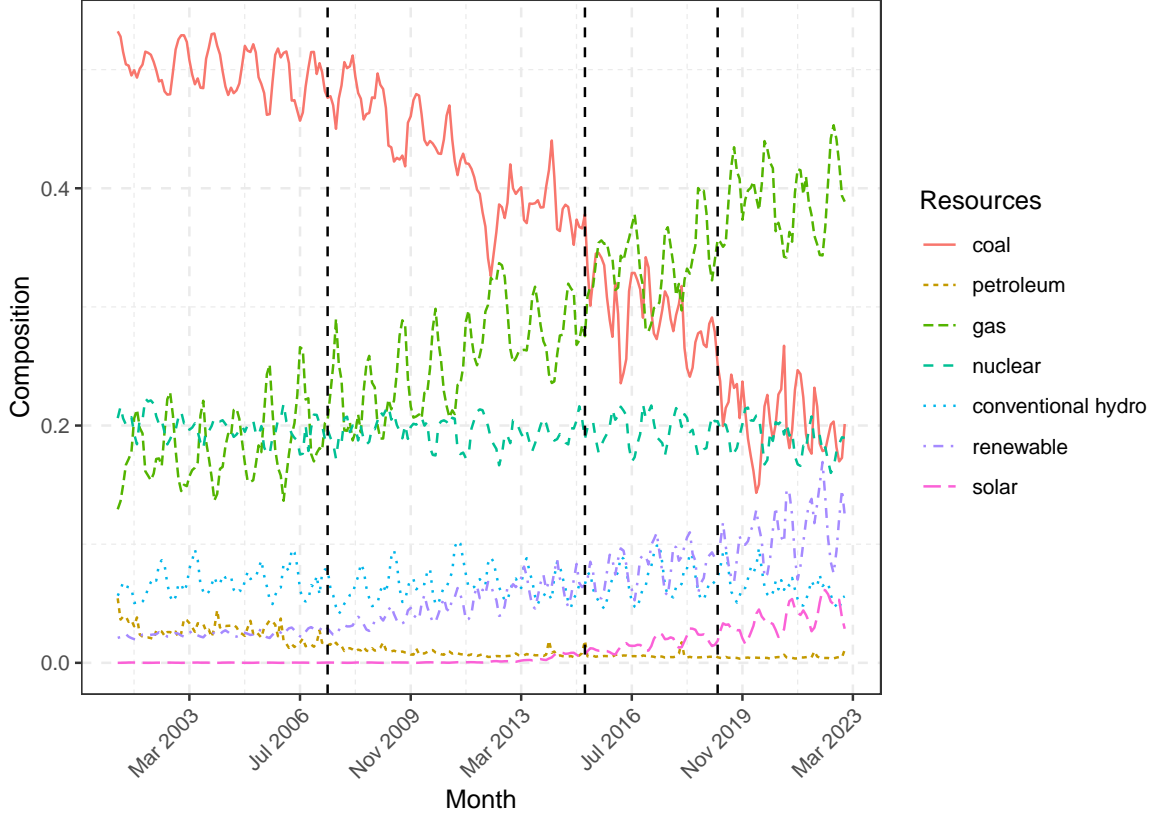


Figure 12: Multiple change points detected for the U.S. electricity generation data. The change points, indicated by the vertical black dashed lines, are at months: May 2007, February 2015 and February 2019.

6 Conclusion

We introduce a nonparametric change point detection method, denoted as dist-CP, designed for random objects taking values in general metric spaces. dist-CP is based solely on pairwise distances and is tuning parameter-free, making it an appealing choice for practitioners working with complex data who seek a straightforward application without the burden of specifying additional parameters except for interval cut-offs where change points are presumed absent. This stands in contrast to other existing approaches for change point detection in metric space data, which typically necessitate parameter choices such as similarity graph selection in graph-CP and kernel and bandwidth selection in kernel-CP. We derive the asymptotic distribution of the test statistic of dist-CP under H_0 to ensure type I error control and establish the large sample consistency of the test and the estimated change points under contiguous alternatives. We extend all theoretical guarantees to the practicable permutation approximations of the null distribution. Comprehensive simulations across various scenarios, spanning random vectors, distributional data, and networks, showcase the efficacy of dist-CP in many challenging settings, including scale

and tail probability changes in Gaussian random vectors and preferential attachment changes in random networks. We study the extension of dist-CP to multiple change point scenarios by combining it with seeded binary segmentation. The data applications lead to insightful findings in the U.S. electricity generation compositions timeline and in the bluetooth proximity networks of the MIT reality mining experiment. With its versatility and minimal parameter requirements dist-CP has the potential for widespread application across various domains as long as distances can be defined between the data elements.

References

- Aminikhanghahi, S. and Cook, D. J. (2017). A survey of methods for time series change point detection. *Knowledge and information systems*, 51(2):339–367.
- Arlot, S., Celisse, A., and Harchaoui, Z. (2019). A kernel multiple change-point algorithm via model selection. *Journal of Machine Learning Research*, 20(162):1–56.
- Barabási, A.-L. and Albert, R. (1999). Emergence of scaling in random networks. *science*, 286(5439):509–512.
- Barassi, M., Horvath, L., and Zhao, Y. (2020). Change-point detection in the conditional correlation structure of multivariate volatility models. *Journal of Business & Economic Statistics*, 38(2):340–349.
- Barnett, I. and Onnela, J.-P. (2016). Change point detection in correlation networks. *Scientific reports*, 6(1):18893.
- Billera, L. J., Holmes, S. P., and Vogtmann, K. (2001). Geometry of the space of phylogenetic trees. *Advances in Applied Mathematics*, 27(4):733–767.
- Carlstein, E. G., Siegmund, D., et al. (1994). Change-point problems. IMS.
- Chakraborty, S. and Zhang, X. (2021). High-dimensional change-point detection using generalized homogeneity metrics. *arXiv preprint arXiv:2105.08976*.
- Chang, W.-C., Li, C.-L., Yang, Y., and Póczos, B. (2019). Kernel change-point detection with auxiliary deep generative models. In *International Conference on Learning Representations*.
- Chen, H. and Chu, L. (2023). Graph-based change-point analysis. *Annual Review of Statistics and Its Application*, 10:475–499.
- Chen, H. and Zhang, N. (2015). Graph-based change-point detection. *The Annals of Statistics*, 43(1):139–176.
- Chen, J., Bittinger, K., Charlson, E. S., Hoffmann, C., Lewis, J., Wu, G. D., Collman, R. G., Bushman, F. D., and Li, H. (2012). Associating microbiome composition with environmental covariates using generalized UniFrac distances. *Bioinformatics*, 28(16):2106–2113.

- Chen, J. and Gupta, A. K. (2012). Parametric statistical change point analysis: with applications to genetics, medicine, and finance. *Springer*.
- Chen, T., Park, Y., Saad-Eldin, A., Lubberts, Z., Athreya, A., Pedigo, B. D., Vogelstein, J. T., Puppo, F., Silva, G. A., Muotri, A. R., et al. (2023). Discovering a change point in a time series of organoid networks via the iso-mirror. *arXiv preprint arXiv:2303.04871*.
- Chu, L. and Chen, H. (2019). Asymptotic distribution-free change-point detection for multivariate and non-euclidean data. *The Annals of Statistics*, 47(1):382–414.
- Chung, E. and Romano, J. P. (2016). Asymptotically valid and exact permutation tests based on two-sample u-statistics. *Journal of Statistical Planning and Inference*, 168:97–105.
- Chung, T. and Maisto, S. A. (2006). Relapse to alcohol and other drug use in treated adolescents: Review and reconsideration of relapse as a change point in clinical course. *Clinical Psychology Review*, 26(2):149–161.
- Cribben, I. and Yu, Y. (2017). Estimating whole-brain dynamics by using spectral clustering. *Journal of the Royal Statistical Society Series C: Applied Statistics*, 66(3):607–627.
- Csörgő, M. and Horváth, L. (1997). Limit theorems in change-point analysis. (*No Title*).
- Dehning, J., Zierenberg, J., Spitzner, F. P., Wibral, M., Neto, J. P., Wilczek, M., and Priesemann, V. (2020). Inferring change points in the spread of covid-19 reveals the effectiveness of interventions. *Science*, 369(6500):eabb9789.
- Dubey, P., Chen, Y., and Müller, H.-G. (2022). Depth profiles and the geometric exploration of random objects through optimal transport. *arXiv preprint arXiv:2202.06117*.
- Dubey, P., Chen, Y., and Müller, H.-G. (2023). A new two-sample test for random objects based on distance profiles. *arXiv preprint arXiv:XXXXX*.
- Dubey, P. and Müller, H.-G. (2020). Fréchet change-point detection. *The Annals of Statistics*, 48(6):3312 – 3335.
- Eagle, N. and Pentland, A. (2006). Reality mining: Sensing complex social systems. *Personal Ubiquitous Comput.*, 10(4):255–268.
- Enikeeva, F. and Harchaoui, Z. (2019). High-dimensional change-point detection under sparse alternatives.
- Erdman, C. and Emerson, J. W. (2008). A fast bayesian change point analysis for the segmentation of microarray data. *Bioinformatics*, 24(19):2143–2148.
- Fryzlewicz, P. (2014). Wild binary segmentation for multiple change-point detection. *The Annals of Statistics*, 42(6):2243 – 2281.

- Garreau, D. and Arlot, S. (2018). Consistent change-point detection with kernels. *Electronic Journal of Statistics*, 12:4440–4486.
- Ginestet, C. E., Li, J., Balachandran, P., Rosenberg, S., and Kolaczyk, E. D. (2017). Hypothesis testing for network data in functional neuroimaging. *The Annals of Applied Statistics*, pages 725–750.
- Gloor, G. B., Wu, J. R., Pawlowsky-Glahn, V., and Egozcue, J. J. (2016). It’s all relative: analyzing microbiome data as compositions. *Annals of epidemiology*, 26(5):322–329.
- Harchaoui, Z. and Cappé, O. (2007). Retrospective mutiple change-point estimation with kernels. In *2007 IEEE/SP 14th Workshop on Statistical Signal Processing*, pages 768–772. IEEE.
- Harchaoui, Z., Moulines, E., and Bach, F. (2008). Kernel change-point analysis. *Advances in neural information processing systems*, 21.
- Holdren, J. P. and Simon, B. (2016). Renewable electricity progress accelerated in 2015.
- Holmes, S. (2003). Statistics for phylogenetic trees. *Theoretical population biology*, 63(1):17–32.
- Horváth, L., Kokoszka, P., and Wang, S. (2021). Monitoring for a change point in a sequence of distributions. *The Annals of Statistics*, 49(4):2271–2291.
- Jaiswal, R., Lohani, A., and Tiwari, H. (2015). Statistical analysis for change detection and trend assessment in climatological parameters. *Environmental Processes*, 2:729–749.
- James, B., James, K. L., and Siegmund, D. (1987). Tests for a change-point. *Biometrika*, 74(1):71–83.
- James, B., James, K. L., and Siegmund, D. (1992). Asymptotic approximations for likelihood ratio tests and confidence regions for a change-point in the mean of a multivariate normal distribution. *Statistica Sinica*, 2(1):69–90.
- Jeon, J. M. and Park, B. U. (2020). Additive regression with Hilbertian responses. *The Annals of Statistics*, 48(5):2671–2697.
- Jeong, S.-O., Pae, C., and Park, H.-J. (2016). Connectivity-based change point detection for large-size functional networks. *Neuroimage*, 143:353–363.
- Jiang, F., Zhao, Z., and Shao, X. (2023). Time series analysis of covid-19 infection curve: A change-point perspective. *Journal of econometrics*, 232(1):1–17.
- Jirak, M. (2015). Uniform change point tests in high dimension. *The Annals of Statistics*, 43(6):2451 – 2483.
- Jones, C. and Harchaoui, Z. (2020). End-to-end learning for retrospective change-point estimation. In *30th IEEE International Workshop on Machine Learning for Signal Processing*.

- Kim, J., Rosenberg, N. A., and Palacios, J. A. (2020). Distance metrics for ranked evolutionary trees. *Proceedings of the National Academy of Sciences*, 117(46):28876–28886.
- KJ, P., Singh, N., Dayama, P., Agarwal, A., and Pandit, V. (2021). Change point detection for compositional multivariate data. *Applied Intelligence*, pages 1–26.
- Kolaczyk, E. D., Lin, L., Rosenberg, S., Walters, J., and Xu, J. (2020). Averages of unlabeled networks: Geometric characterization and asymptotic behavior. *The Annals of Statistics*, 48(1):514–538.
- Kossinets, G. and Watts, D. J. (2006). Empirical analysis of an evolving social network. *science*, 311(5757):88–90.
- Kovács, S., Bühlmann, P., Li, H., and Munk, A. (2023). Seeded binary segmentation: a general methodology for fast and optimal changepoint detection. *Biometrika*, 110(1):249–256.
- Kwon, D., Vannucci, M., Song, J. J., Jeong, J., and Pfeiffer, R. M. (2008). A novel wavelet-based thresholding method for the pre-processing of mass spectrometry data that accounts for heterogeneous noise. *Proteomics*, 8(15):3019–3029.
- Lavielle, M. and Teyssiere, G. (2007). Adaptive detection of multiple change-points in asset price volatility. In *Long memory in economics*, pages 129–156. Springer.
- Li, J. (2020). Asymptotic distribution-free change-point detection based on interpoint distances for high-dimensional data. *Journal of Nonparametric Statistics*, 32(1):157–184.
- Li, S., Xie, Y., Dai, H., and Song, L. (2015). M-statistic for kernel change-point detection. In Cortes, C., Lawrence, N., Lee, D., Sugiyama, M., and Garnett, R., editors, *Advances in Neural Information Processing Systems*, volume 28. Curran Associates, Inc.
- Lindquist, M. A., Waugh, C., and Wager, T. D. (2007). Modeling state-related fmri activity using change-point theory. *NeuroImage*, 35(3):1125–1141.
- Liu, H., Gao, C., and Samworth, R. J. (2021). Minimax rates in sparse, high-dimensional change point detection. *The Annals of Statistics*, 49(2):1081 – 1112.
- Londschien, M., Bühlmann, P., and Kovács, S. (2023). Random forests for change point detection. *Journal of Machine Learning Research*, 24(216):1–45.
- Lund, R. B., Beaulieu, C., Killick, R., Lu, Q., and Shi, X. (2023). Good practices and common pitfalls in climate time series changepoint techniques: A review. *Journal of Climate*, pages 1–38.
- Lung-Yut-Fong, A., Lévy-Leduc, C., and Cappé, O. (2015). Homogeneity and change-point detection tests for multivariate data using rank statistics. *Journal de la Société Française de Statistique*, 156(4):133–162.

- Lyons, R. (2013). Distance covariance in metric spaces. *Annals of Probability*, 41(5):3284–3305.
- Madrid Padilla, O. H., Yu, Y., Wang, D., and Rinaldo, A. (2021). Optimal nonparametric change point analysis.
- Madrid Padilla, O. H., Yu, Y., Wang, D., and Rinaldo, A. (2022). Optimal nonparametric multivariate change point detection and localization. *IEEE Transactions on Information Theory*, 68(3):1922–1944.
- Matabuena, M., Petersen, A., Vidal, J. C., and Gude, F. (2021). Glucodensities: A new representation of glucose profiles using distributional data analysis. *Statistical methods in medical research*, 30(6):1445–1464.
- Matteson, D. S. and James, N. A. (2014). A nonparametric approach for multiple change point analysis of multivariate data. *Journal of the American Statistical Association*, 109(505):334–345.
- Muggeo, V. M. R. and Adelfio, G. (2010). Efficient change point detection for genomic sequences of continuous measurements. *Bioinformatics*, 27(2):161–166.
- Nie, L. and Nicolae, D. L. (2021). Weighted-graph-based change point detection.
- Nie, Y., Wang, L., and Cao, J. (2017). Estimating time-varying directed gene regulation networks. *Biometrics*, 73(4):1231–1242.
- Niu, Y. S., Hao, N., and Zhang, H. (2016). Multiple change-point detection: a selective overview. *Statistical Science*, pages 611–623.
- Oliver, J. L., Carpena, P., Hackenberg, M., and Bernaola-Galván, P. (2004). Isofinder: computational prediction of isochores in genome sequences. *Nucleic acids research*, 32(suppl_2):W287–W292.
- Page, E. (1955). A test for a change in a parameter occurring at an unknown point. *Biometrika*, 42(3/4):523–527.
- Page, E. S. (1954). Continuous inspection schemes. *Biometrika*, 41(1/2):100–115.
- Peel, L. and Clauset, A. (2015a). Detecting change points in the large-scale structure of evolving networks. In *Proceedings of the AAAI Conference on Artificial Intelligence*, volume 29.
- Peel, L. and Clauset, A. (2015b). Detecting change points in the large-scale structure of evolving networks. In *Proceedings of the Twenty-Ninth AAAI Conference on Artificial Intelligence*, AAAI’15, page 2914–2920. AAAI Press.
- Picard, F., Lebarbier, E., Hoebeke, M., Rigail, G., Thiam, B., and Robin, S. (2011). Joint segmentation, calling, and normalization of multiple cgh profiles. *Biostatistics*, 12(3):413–428.

- Sato, H., Hirakawa, A., and Hamada, C. (2016). An adaptive dose-finding method using a change-point model for molecularly targeted agents in phase i trials. *Statistics in medicine*, 35(23):4093–4109.
- Sharpe, J. D., Hopkins, R. S., Cook, R. L., and Striley, C. W. (2016). Evaluating google, twitter, and wikipedia as tools for influenza surveillance using bayesian change point analysis: a comparative analysis. *JMIR public health and surveillance*, 2(2):e5901.
- Shen, J. J. and Zhang, N. R. (2012). Change-point model on nonhomogeneous Poisson processes with application in copy number profiling by next-generation DNA sequencing. *The Annals of Applied Statistics*, 6(2):476 – 496.
- Shi, X., Wu, Y., and Rao, C. R. (2017). Consistent and powerful graph-based change-point test for high-dimensional data. *Proceedings of the National Academy of Sciences*, 114(15):3873–3878.
- Sporns, O. (2022). Structure and function of complex brain networks. *Dialogues in clinical neuroscience*.
- Srivastava, M. S. and Worsley, K. J. (1986). Likelihood ratio tests for a change in the multivariate normal mean. *Journal of the American Statistical Association*, 81(393):199–204.
- Stoehr, C., Aston, J. A., and Kirch, C. (2021). Detecting changes in the covariance structure of functional time series with application to fmri data. *Econometrics and Statistics*, 18:44–62.
- Tavakoli, S., Pigoli, D., Aston, J. A., and Coleman, J. S. (2019). A spatial modeling approach for linguistic object data: Analyzing dialect sound variations across great britain. *Journal of the American Statistical Association*, 114(527):1081–1096.
- Thies, S. and Molnár, P. (2018). Bayesian change point analysis of bitcoin returns. *Finance Research Letters*, 27:223–227.
- Truong, C., Oudre, L., and Vayatis, N. (2020). Selective review of offline change point detection methods. *Signal Processing*, 167:107299.
- Van Der Vaart, A. W., Wellner, J. A., van der Vaart, A. W., and Wellner, J. A. (1996). *Weak convergence*. Springer.
- Wang, D., Yu, Y., and Rinaldo, A. (2020). Univariate mean change point detection: Penalization, cusum and optimality.
- Wang, D., Yu, Y., and Rinaldo, A. (2021). Optimal change point detection and localization in sparse dynamic networks.
- Wang, R., Zhu, C., Volgushev, S., and Shao, X. (2022). Inference for change points in high-dimensional data via selfnormalization. *The Annals of Statistics*, 50(2):781–806.

- Wang, T. and Samworth, R. J. (2018). High dimensional change point estimation via sparse projection. *Journal of the Royal Statistical Society Series B: Statistical Methodology*, 80(1):57–83.
- Wang, Y., Chakrabarti, A., Sivakoff, D., and Parthasarathy, S. (2017). Fast change point detection on dynamic social networks. *arXiv preprint arXiv:1705.07325*.
- Zhang, N. R., Siegmund, D. O., Ji, H., and Li, J. Z. (2010). Detecting simultaneous changepoints in multiple sequences. *Biometrika*, 97(3):631–645.